Online Appendix for the following *JACC: Cardiovascular Imaging* article

TITLE: Induction of Regression of Inflammation in Atherosclerosis by the LXR Agonist R211945: A Multimodality Noninvasive Assessment and Comparison With Atorvastatin

AUTHORS: Esad Vucic, MD, Claudia Calcagno, MD, PHD, Stephen D. Dickson, MS, James H.F. Rudd, MD, PHD, Katsumi Hayashi, MD, Jan Bucerius, MD, Erin Moshier, MS, Jessica S. Mounessa, BS, Michelle Roytman, BS, Matthew J. Moon, BS, James Lin, MS, Sarayu Ramachandran, MS, Tatsuo Tanimoto, PHD, Karen Brown PHD, Masakatsu Kotsuma, PHD, Sotirios Tsimikas, MD, Edward A. Fisher, MD, PHD, Klaas Nicolay, PHD, Valentin Fuster , MD, PHD, Zahi A. Fayad, PHD

APPENDIX

Methods-Manuscript

Blood Analysis

Blood sampling was performed before diet initiation and at 4,5 and 7 months after diet initiation. Animals were fasted for 12 hours prior to blood collection and the obtained serum was analyzed using commercial kits for cholesterol, triglycerides, glucose (Wako Chemicals) and insulin (Millipore). Plasma levels of R211945 and atorvastatin were determined by mass spectrometry (Taylor Technology, Princeton, NJ)

Immunohistology

Standard immunohistochemistry techniques were used to quantify macrophages and neovessels in the vessel wall. Macrophages-rich areas were identified using RAM-11 staining and expressed as a fraction of the media-intimal area (macrophage density) per slice. The average macrophages density per animal was used in the statistical analysis. Areas of smooth muscle actin, apolipoprotein B-100 and oxidized phospholipids were evaluated in a similar fashion. Neovessels were identified using CD-31 staining as previously described, on the histological sections matching with the imaged DCE slice (1).

Statistical Power

Prior to begin of the study we performed calculations for the sample size for FDG-PET/CT imaging on data available from our group (2). We obtained the statistical standard deviation for SUV max- values pre- and post- treatment (±0.03 and ±0.1, respectively) and the observed treatment effect (reduction in SUV of about 28%). Based on this data and other published data in rabbit (3), we estimated a 25% to 30% reduction in SUV for our study. The resulting sample size was between n=3 and n=4 , to have 80% power to detect a difference based on a 2-sample paired t-test (2-sided) with 1-beta (power) =80% power and alpha= 5%. We also took into account data from a human FDG-PET/CT reproducibility study (4). Based on this data and a 25-30% estimated therapeutic effect, the sample size is between n=5 to n=7 , to have 80% power to detect a difference based on a 2-sample paired t-test (2-sided) with 1-beta (power) =80% power and alpha= 5%.

In terms of DCE-MRI, we based the sample size calculation on a reproducibility study in the same animal model used herein(5). We assumed a similar reduction for AUC as for SUV of

about 25%-30% upon treatment. The resulting sample size is between n=5 to n=7, to have 80% power to detect a difference based on a 2-sample paired t-test (2-sided) with 1-beta (power) =80% power and alpha= 5%.

Statistical Analysis—Linear Mixed Model

Continuous DCE-MRI and PET/CT outcomes were modeled as linear functions of time by using a linear mixed model. This approach allowed estimating the regression equation for each group, while accounting at the same time for the correlation between repeated measurements in each rabbit over time. In the case of PET outcomes, the models were weighted by the number of slices analyzed in each animal. In addition we tested for differences among the slopes of treatment and control groups estimated by linear regression equations by including an interaction term between treatment group and time was included in each mixed model along with both main effects. If the interaction term was found to be statistically significant then pair-wise comparisons of treatment group slopes were estimated. To adjust for multiple comparisons we used the Bonferroni-Holm step down procedure (6). All statistical analyses were performed using Proc Mixed in SAS Version 9.2 (7).

Methods-Supplement

Quantitative PCR (qPCR) of ABCA1

Quantitative ABCA1-PCR analysis was performed (Beckman Coulter Genomics, Houston, TX).Total RNA was isolated from PAXgene® (Becton Dickinson) blood tubes using Promega's PAXgene Blood RNA Kit (Promega) ,then visualized by agarose gel

and quantitated by a Nanodrop spectrophotometer (Thermo Fisher). All samples were then further treated with DNase, visualized by agarose gel and quantitated by Nanodrop again. Each RNA sample was reverse transcribed to cDNA using a Superscript II (Gibco/BRL). Each cDNA sample was tested by qPCR with rabbit ABCA1 and β actin.

qPCR

The real-time PCR mixture for each gene (28 μL per sample), including 0.15 μL of 10 μM primer 1 (Sigma-Aldrich Co.), 0.15 μL of 10 μM primer 2 (Sigma-Aldrich), probe (final 200 nM) (Applied Biosystems), 15 μL of TaqMan Universal PCR Master Mix (Applied Biosystems) and water, was pipetted into the wells of a 96-well reaction plate. Then, 2 μL of each cDNA solution or standard solution was added. Real-time PCR reaction, with conditions set at 50°C for 2 min, at 95°C for 10 min and 40 or 50 repeated-cycles at 95°C for 15 sec and at 60°C for 1 min, was performed using ABI PRISM 7700 Sequence Detector (Applied Biosystems). ABCA1 expression levels were then plotted relative to β-actin content.

The sequences of primers and probes are described below.

β-actin:

probe : FAM- 5' CTGGCCTCGCTCTCCACCTTCCA 3'-TAMRA

primer 1 : 5' GGATCGGCGGCTCCAT 3'

primer 2 : 5' CATACTCCTGCTTGCTGATCCA 3'

ABCA1:

probe : FAM- 5' AGAAGTTGGCAAGGTTGGTGAGTG 3' -TAMRA

primer 1 : 5' TGGGAGAGAGCATGTGGAGTT 3'

primer 2 : 5' GCCCAGTTTGCGAATTGC 3'

Linear Regression Analysis

Macrophages density and neovessels as quantified by histology were correlated with both DCE-MRI and PET/CT outcomes using Pearson testing after normality of the data was established. Five animals from each group were used.

Supplemental results

SUV Correlates With Tissue Macrophage Content and AUC Correlates With Neovascularization

We found a strong positive correlation between maximal SUV and macrophages (r^2 = 0.86, $p < 0.0001$) and between AUC_{1min} and neovessels ($r^2 = 0.51$, $p = 0.004$) **(Supplemental Figure 1 A and B)** consistent with previous studies (1,8).

R211945 Induces ABCA1 Expression

We evaluated ABCA1 expression, as the major LXR agonist target, for all groups **(Supplemental Figure 2)**. R211945 treatment lead to an increase in ABCA1 expression in peripheral blood of 101% at 1 month ($p = 0.007$ vs. control) and 88% at 3 months ($p = 0.01$ vs. control) whereas atorvastatin treatment led to a decrease of 17% at 1 month ($p = 0.36$ vs. control) and 30% at 3 months ($p = 0.01$ vs. control), consistent with previous studies (8,9). Vehicle treatment did not result in an increase in ABCA1 expression.

Figure Legends

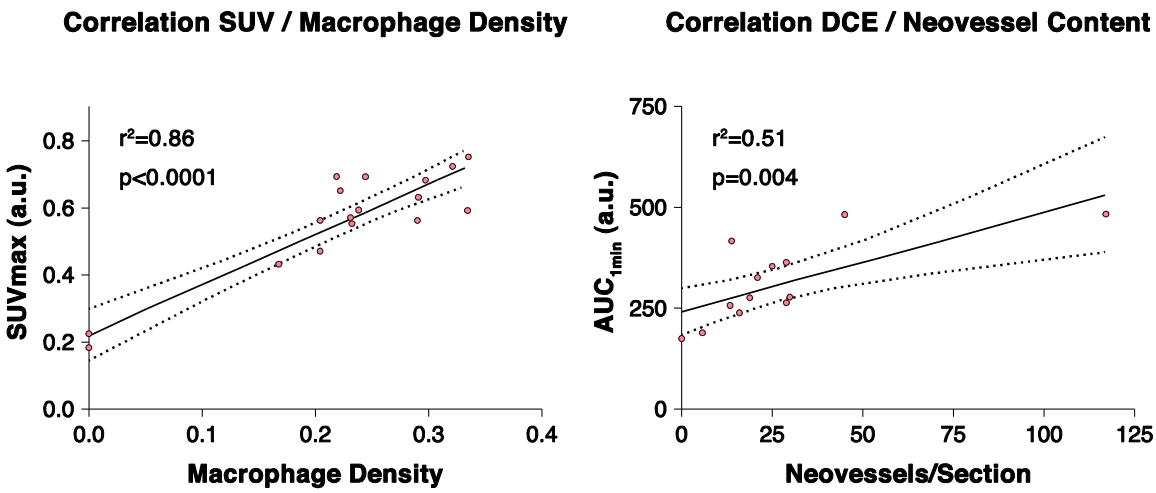

Supplemental Figure 1. Regression Analysis

Left. Correlation between average maximal ($\overline{max}$) standard uptake value ($SUV\overline{max}$) generated from FDG-PET/CT imaging and macrophage density (stained area/intimal area) from histological staining. **Right.** Correlation between mean AUC_{1min} generated from DCE-MRI imaging and neovessel count per histological section. Black line, regression line; dashed line, 95% confidence interval.

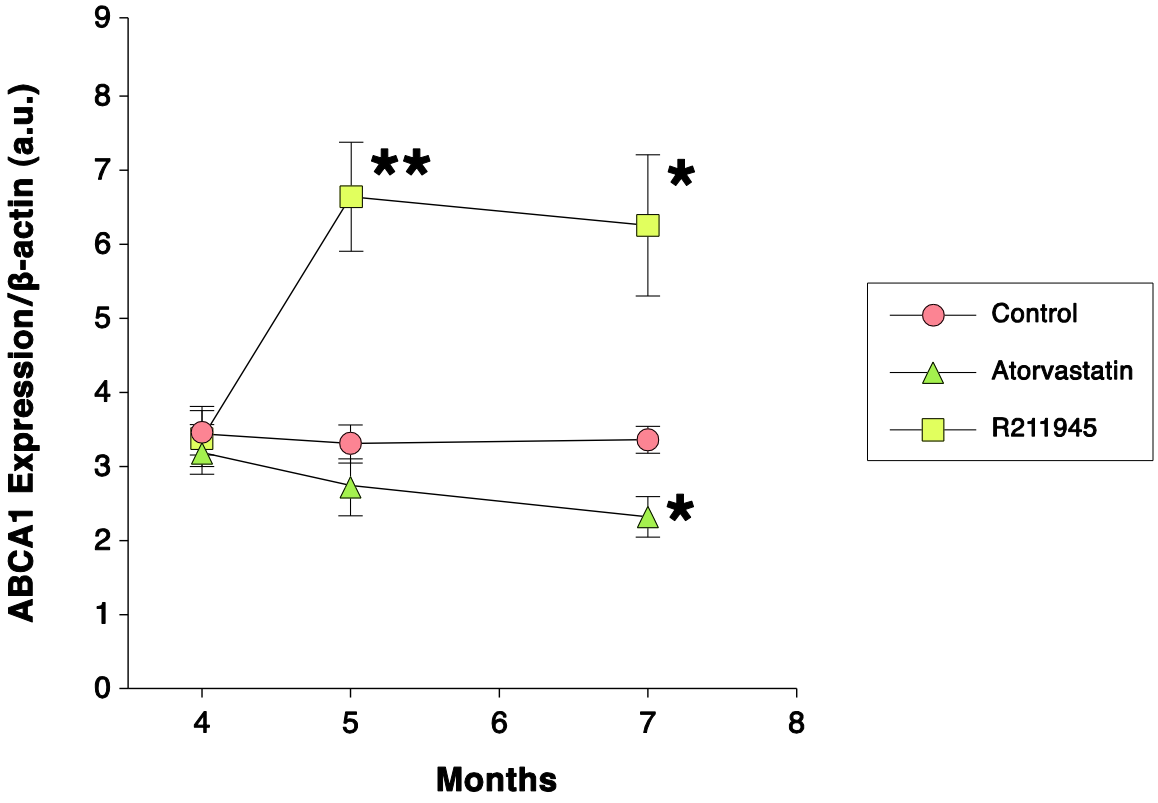

Supplemental Figure 2. Relative ABCA1 expression

RNA expression in peripheral blood relative to β-actin at baseline (total 4 month), 1 month (total 5 month) and 3 month (total 7 month); *$p < 0.05$, **$p < 0.01$ control versus treatment group.

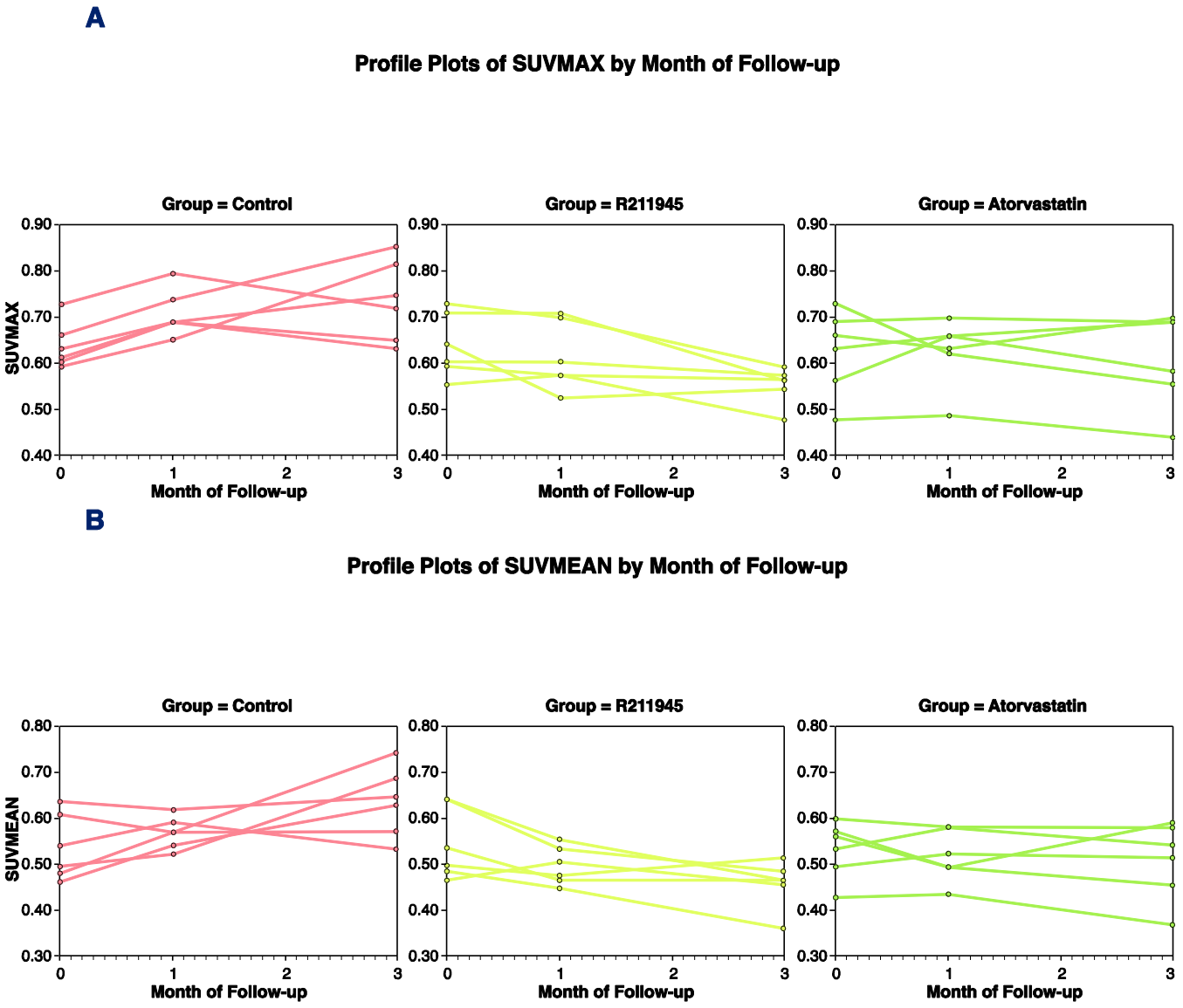

Supplemental Figure 3. Individual SUV-values

SUVmax and SUVmean values plotted over time (Figure 3A and B).

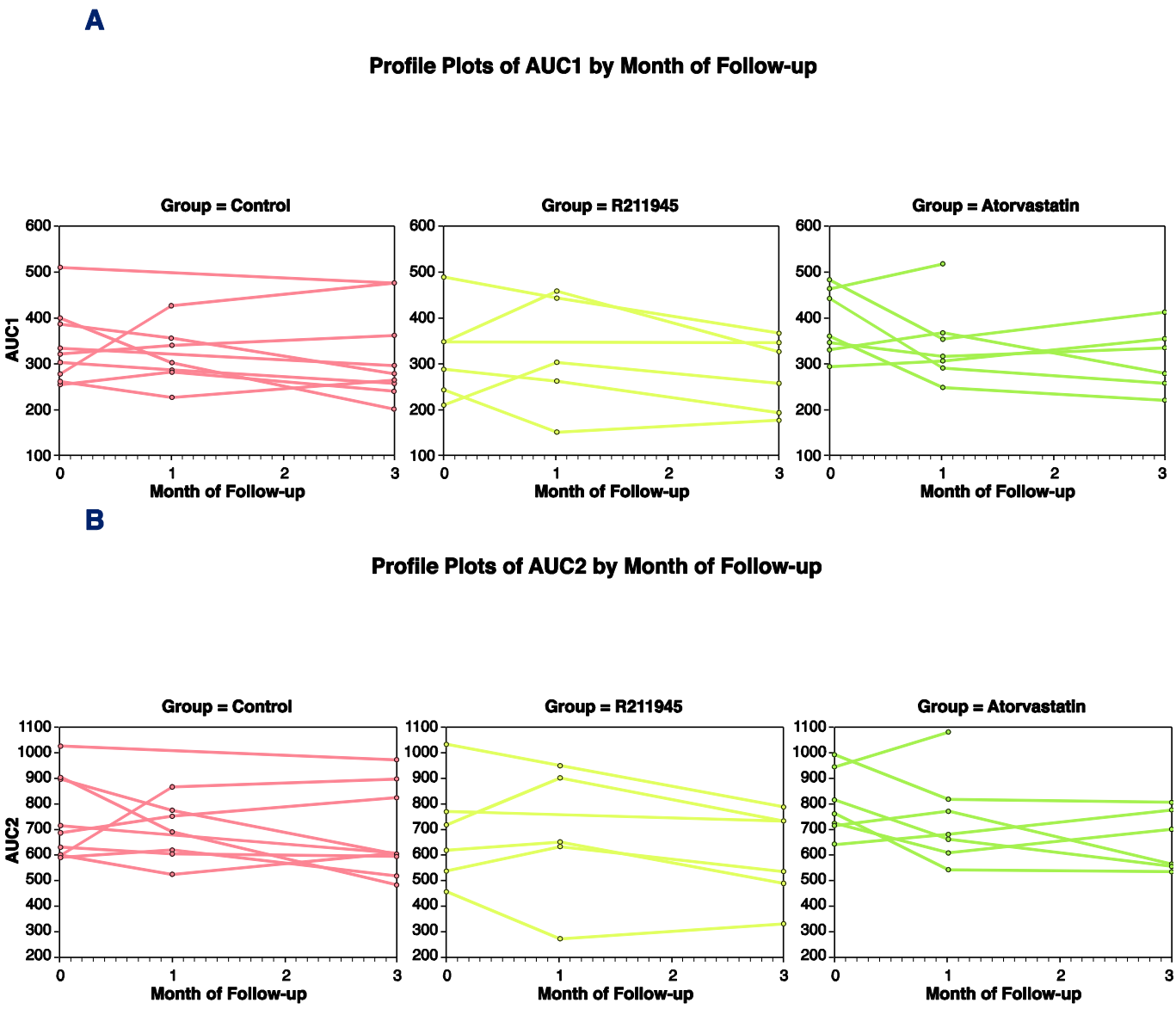

Supplemental Figure 4. Individual AUC-values

Individual, per animal, AUC 1 min (AUC1) and AUC 2 min (AUC2) values plotted over time (Figure 4A and B).

REFERENCES

1. Calcagno C, Cornily JC, Hyafil F, et al. Detection of neovessels in atherosclerotic plaques of rabbits using dynamic contrast enhanced MRI and 18F-FDG PET. Arterioscler Thromb Vasc Biol 2008;28:1311-7.
2. Lobatto ME, Fayad ZA, Silvera S, et al. Multimodal clinical imaging to longitudinally assess a nanomedical anti-inflammatory treatment in experimental atherosclerosis. Molecular Pharmaceutics 2010;7:2020-9.
3. Ogawa M, Magata Y, Kato T, et al. Application of 18F-FDG PET for monitoring the therapeutic effect of antiinflammatory drugs on stabilization of vulnerable atherosclerotic plaques. J Nucl Med 2006;47:1845.
4. Rudd JH, Myers KS, Bansilal S, et al. (18)Fluorodeoxyglucose positron emission tomography imaging of atherosclerotic plaque inflammation is highly reproducible: implications for atherosclerosis therapy trials. J Am Coll Cardiol 2007;50:892-6.
5. Calcagno C, Vucic E, Mani V, Goldschlager G, Fayad ZA. Reproducibility of black blood dynamic contrast-enhanced magnetic resonance imaging in aortic plaques of atherosclerotic rabbits. Journal of Magnetic Resonance Imaging 2010;32:191-198.
6. Holm S. A Simple sequentially rejective multiple test procedure. Scandinavian Journal of Statistics 1979;6:65-70.
7. Littell Ramon C. GAM, Walter W. Stroup, Russell D. Wolfinger. SAS System for Mixed Models. Cary, NC: SAS Institute Inc., 1996.

8. Vucic E, Dickson SD , Calcagno C, Rudd JHF, Moshier E, Hayashi K, Mounessa JS, Roytman M, Moon MJ, Lin J, Tsimikas S, Fisher EA, Nicolay K, Fuster V, Fayad ZA. Pioglitazone modulates vascular inflammation in atherosclerotic rabbits monitored non-invasively with 18F-fluorodeoxyglucose-PET/CT and black blood dynamic contrast enhanced-MRI. J Am Coll Cardiol Img 2011;In press.